Multifractal analysis of the spatial distribution of the film surfaces with different roughening mechanisms

J. G. Hou,[1] Wang Yan,[1] Xia Rui,[1] Zhu Xiaoguang,[2] Wang Haiqian,[1] and Z. Q. Wu[1]
[1]*Structure Research Laboratory and Hefei Advanced Research Institute, University of Science and Technology of China, Hefei, Anhui 230026, China*
[2]*Solid State Institute, Chinese Academy of Sciences, Hefei, Anhui 230026, China*
(Received 31 December 1997)

Thin films of C_{60}/Ag were prepared by codeposition of C_{60} and Ag onto (001) NaCl substrates. The surface roughness depends strongly on the substrate temperature, and a transition from kinetically roughening to thermally roughening was observed by using atomic force microscopy. Multifractal spectra of the film surfaces have been studied in the length scale of 30 nm to 5 μm. Compared with the conventional root-mean-square method, the multifractal spectrum provides more information about the spatial distribution of the surface roughness. [S1063-651X(98)06908-6]

PACS number(s): 68.55.−a, 68.35.Bs, 05.40.+j, 05.70.Ln

I. INTRODUCTION

The surface roughness is fundamental for several physical properties and physical phenomena on a solid surface. However, the surface roughness is difficult to quantify since it is hard to describe mathematically. Several methods have been used to quantitatively analyze the surface roughness, such as the peak density method and the root-mean-square (rms) method [1]. Recently, fractal analysis is of growing use in surface science, because the scaling concept simplifies significantly the characterization of a nonequilibrium surface [2–5]. But the single fractal dimension can only provide information about the average global roughness of a measured surface. The concept of multifractal can be well applied in quantitatively characterizing complex geometric shapes or singular distributions of physical parameters, such as material fracture and chemical reaction on a solid surface [6,7], growth probability distribution of diffusion-limited aggregation (DLA) [8], and distribution of secondary-electron emission sites on a solid surface [9]. For the surface of solid-on-solid growth, the results of computer simulations [10,11] indicated that the rough surface can also be characterized by the multifractal spectra. In this paper we have applied the method to C_{60}/Ag films which have interesting physical and structural properties [12,13]. The films with different surface roughness were prepared at different substrate temperatures (T_s) with the same deposition rate. It is found that the spatial distribution of the surface roughness can be well described by multifractal analysis. The width and the height of the bell-shaped spectra increase with the increasing of surface roughness. Moreover, the multifractal spectra of the low temperature roughening surfaces differ from those of the high temperature roughening surfaces. Our study indicates that multifractal is an effective way for quantitative analysis of nonequilibrium surface roughness.

II. EXPERIMENT

The C_{60}/Ag films were prepared by a two source vapor deposition method at a base pressure of 7×10^{-4} Pa. High purity Ag (>99.999%) and C_{60} (>99.9%) powders were used for evaporation. The deposition rates of metal and fullerene were calibrated with a quartz-crystal thickness monitor. The substrates were freshly cleaved (001) NaCl single crystals, and the substrate temperatures were changed from −50 °C to 160 °C in different film deposition runs. C_{60} and Ag were codeposited onto the substrate with rates of 6 nm/min and 3 nm/min, respectively, and the deposition time is 5 min. After deposition, the topography of the film surface was measured quantitatively by an atomic force microscope (AFM) (Park Autoprobe CP, SiN tip, contact mode). Topographies were collected in the length scale of 5 μm, and every topography of 5 μm^2 scans has 512×512 image pixels. For the crystal structural analysis, some of the substrates were dissolved in distilled water and the films were put on the copper grids. A transmission electron microscope (TEM) (Hitachi-800) was used for the structural characterization.

The rms roughness of the films was obtained from the following formula [1]:

$$\sigma=\left[\frac{\left(\sum_{ij} h_{ij}-\overline{h}\right)^2}{N-1}\right]^{1/2}, \tag{1}$$

where h_{ij} is the height of an image pixel and N is the number of total image pixels. The box-counting method has been adopted in multifractal analysis of the spatial distribution of roughness surfaces. Every AFM topography was divided into a number of square boxes (l, k) with different sizes of ε, where $\varepsilon=2/512,\ldots,2^n/512,\ldots,1$. So the value of ε is less than or equal to 1, and the largest box with size of $\varepsilon=1$ consists of 512×512 image pixels. For size ε, the height distribution of probabilities P_{lk} is defined as

$$p_{lk}=\frac{\sum_{\varepsilon} h_{lk}}{\sum_{1} h_{lk}}, \tag{2}$$

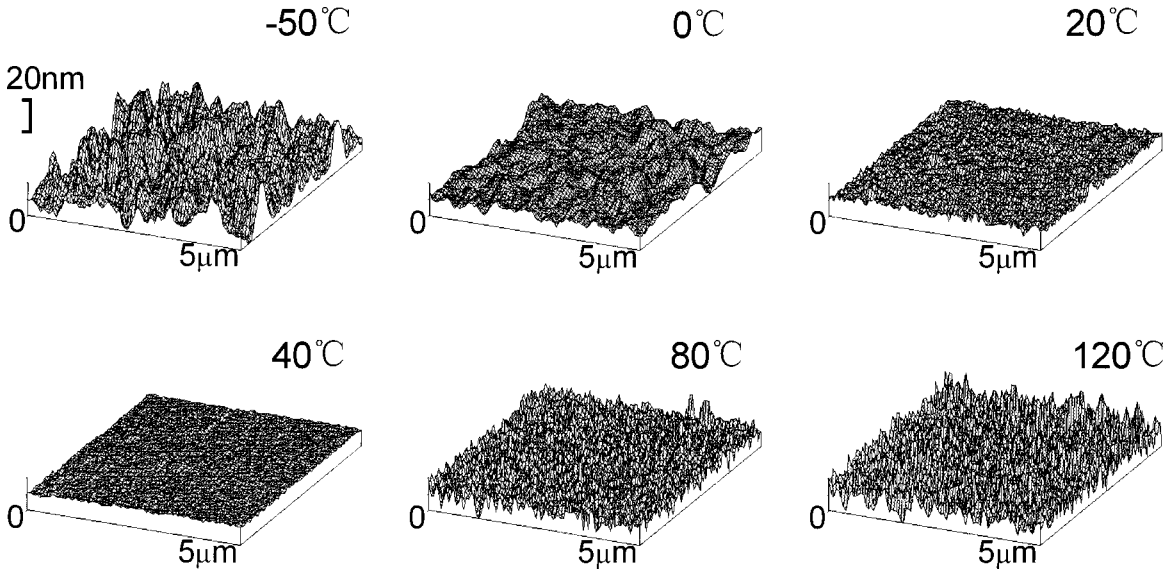

FIG. 1. AFM images of C_{60}/Ag films prepared at different substrate temperatures (T_s).

where h_{lk} is the height of the position determined by l and k, and Σ_ε means the summation of h_{lk} in the box (l, k) of size ε. We can find an exponent (singularity exponent) α [14] as

$$p_{lk}(\varepsilon) \sim \varepsilon^{\alpha}. \tag{3}$$

The partition function can be expressed as a power law with an exponent τ_q (where q is the moment order)

$$\chi_q(\varepsilon) \equiv \sum_{l,k} p_{lk}^q(\varepsilon) = \varepsilon^{\tau(q)} \tag{4}$$

and the generalized fractal dimension Dq,

$$Dq = \frac{1}{q-1} \lim_{\varepsilon \to 0} \frac{\ln \chi(q)}{\ln \varepsilon} = \frac{\tau(q)}{q-1}, \tag{5}$$

then we can obtain multifractal spectrum $f(\alpha)$ by Legendre transformation [14] as follows:

$$\alpha = \frac{d}{dq} \tau(q) \tag{6}$$

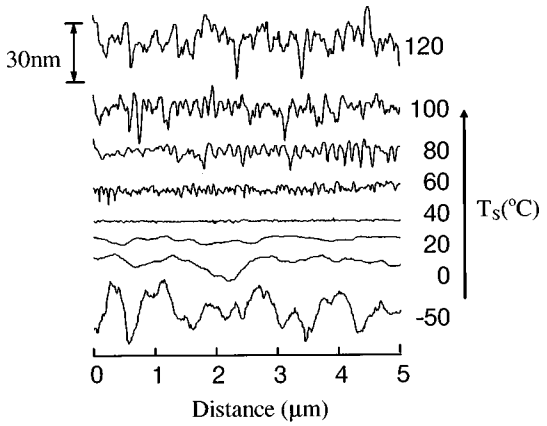

FIG. 2. The height profiles of the films prepared at different substrate temperatures (T_s) along one direction.

and

$$f(\alpha) = \alpha q - \tau(q). \tag{7}$$

III. RESULTS

AFM images of C_{60}/Ag films prepared at different substrate temperatures (T_s) are shown in Fig. 1. The height profiles of the films along one direction are also shown in Fig. 2. From both the AFM images and one dimensional height profiles, we can find that the surface roughness of the films undergoes a transition of rough→smooth→rough when the substrate temperature increases from −50 °C to 120 °C. A very smooth surface was obtained when $T_s = 40$ °C. Figure 3 shows the results of rms roughness (σ) of the films grown at different substrate temperatures. According to the relation between the roughness and the substrate temperature: σ increases with the increasing of temperature or vice versa, samples can be divided into two groups, and $T_s = 40$ °C is the transition temperature of the surface roughness.

Figures 4(a) and 4(b) are two TEM images and electron diffraction patterns of the films prepared at the substrate temperature of −50 °C and 120 °C, respectively. The very dis-

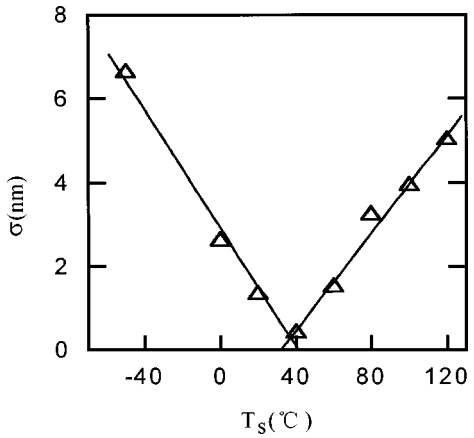

FIG. 3. The rms roughness (σ) of the films grown at different substrate temperatures.

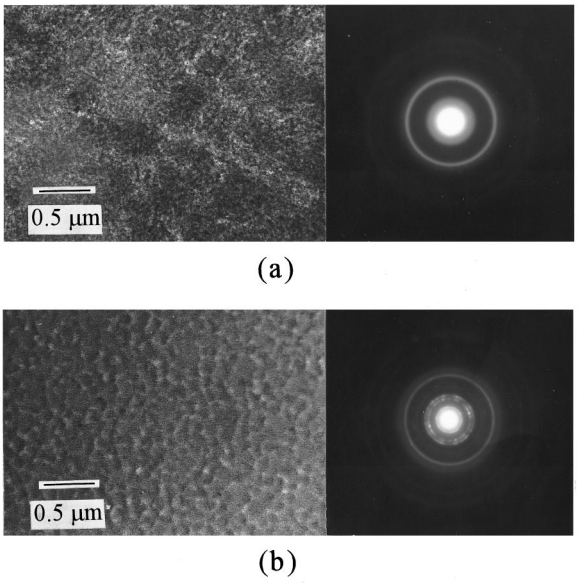

FIG. 4. TEM images and electron diffraction patterns of the films prepared at the substrate temperatures of −50 °C (a) and 120 °C (b).

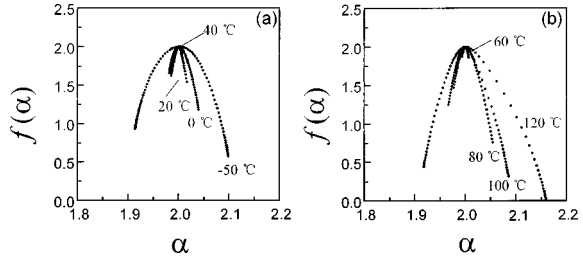

FIG. 5. Multifractal spectra $f(\alpha)$ of the spatial distribution of surface height for the low (a) and high (b) temperature films.

persed diffraction pattern shown in Fig. 4(a) indicates that both C_{60} and Ag are almost amorphous in the low temperature film. Polycrystalline film with very large C_{60} grains was obtained when $T_s = 120$ °C since a spotlike diffraction pattern was observed.

IV. DISCUSSION

In recent years, the nonequilibrium surface roughening mechanism and the transition from the kinetic roughening (at low temperatures or high deposition rate) to the thermal roughening (at high temperatures) have attracted considerable interest [15–17]. Although the nature of the transition is still not very clear, it is evident that the roughening mechanism of low temperatures is not the same as that of high temperatures. From the results of TEM analysis, we can discuss the possible roughening mechanisms in our films: low temperature roughness is due to the random stacking of deposited particles since the surface diffusion is limited by low kinetic energy; while the coalescence effect of grains into a larger island (Oswald ripening) during the crystallization of C_{60} is the main reason for the appearance of rough surfaces at high temperatures. It is noted that for the surfaces with similar rms values, both the topography and the one dimensional height profile shown in Figs. 1 and 2 are quite different. So it is clear that the rms method is unable to distinguish the difference between the kinetic and the thermal roughening surfaces which have very different spatial distribution and microstructure. Figures 5(a) and 5(b) show the multifractal spectra $f(\alpha)$ of the spatial distribution of surface height for the low and high temperature films, respectively. All the $f(\alpha) \sim \alpha$ spectra are bell-like curves though the width and the height of the spectra are dependent on the substrate temperature. We can define the spectrum width $\Delta\alpha$ as $\Delta\alpha = \alpha_{\max} - \alpha_{\min}$, where $\alpha_{\max}$ and $\alpha_{\min}$ are maximum and minimum singularities, respectively. The width represents the range of the height distribution of probabilities. From Figs. 5(a) and 5(b), the relationship between the spectrum width and the roughness can be found. It is evident that the rougher the surface, the wider the spectra width. We also find that the probability distribution range is narrower for the surfaces with small rms roughness, or in other words this result suggests that the height distribution of the smoother surface is more uniform than that of the rougher surface.

The results shown in Fig. 5 indicate that the surface roughness can be well described by the multifractal spectra; a question here is whether multifractal analysis can provide more information than the rms method about the surfaces with different roughening mechanisms. The multifractal spectra shown in Figs. 5(a) and 5(b) are the global spatial distribution of the surfaces in the range of 10 nm to 5 μm, since the value of ε is taken from 2/512 to 1 when calculating the probability distributions. According to the definition, ε is the normalized box size and the largest box ($\varepsilon = 1$) consists of 512×512 image pixels. Next we will study the spatial distribution property of the films in different length scales, for example, the probabilities are calculated in the ranges of $2/512 \leqslant \varepsilon \leqslant 32/512$ and $32/512 \leqslant \varepsilon \leqslant 1$, respec-

TABLE I. Some parameters of the multifractal spectra obtained from the spatial probability distributions calculated in the different length scales: 10 nm to 0.3 μm and 0.3 μm to 5 μm. $\Delta f(\alpha)$ is defined as $\Delta f(\alpha) = f(\alpha)_{\max} - [f(\alpha_{\min}) + f(\alpha_{\max})]/2$.

	$T_s = -50$ °C 10 nm to 0.3 μm	$T_s = 120$ °C 10 nm to 0.3 μm	$T_s = -50$ °C 0.3 μm to 5 μm	$T_s = 120$ °C 0.3 μm to 5 μm
$\alpha_{\min}$	1.976	1.864	1.906	1.989
$\alpha_{\max}$	2.033	2.216	2.096	2.009
$\Delta\alpha$	0.057	0.352	0.190	0.020
$f(\alpha)_{\max}$	2.000	2.000	2.000	2.000
$f(\alpha_{\min})$	1.766	0.046	0.553	1.734
$f(\alpha_{\max})$	1.621	0.385	0.494	1.798
$\Delta f(\alpha)$	0.307	1.785	1.477	0.234

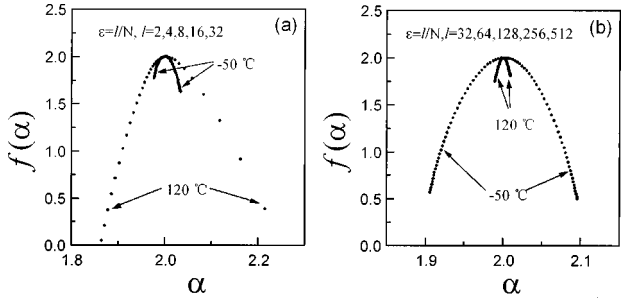

FIG. 6. Multifractal spectra obtained from spatial probability distributions calculated in the different length scales: for scale 10 nm to 0.3 μm (a) and for scale 0.3 μm to 5 μm (b).

tively. We find that the multifractal spectra of the kinetic and the thermal roughening surfaces are quite different if the spatial probability distributions are calculated in the different length scales. Figure 6(a) shows the multifractal spectra of small length scale (10 nm to 0.3 μm) for the two films obtained at -50 °C and 120 °C, respectively. From the figure, we can see that the width and the height of bell spectrum for the low temperature surface are much smaller than those of the high temperature surface. However, this result is reversed when the probabilities were calculated in the larger length scale (0.3 μm to 5 μm) [see Fig. 6(b)]. Some multifractal parameters of the spectra in different length scales are listed in Table I. According to the physical meaning of the parameters discussed above, the results shown in Fig. 6 suggest that in the length scale of 10 nm to 0.3 μm, the spatial distribution of the low temperature surface is more uniform than that of the high temperature surface, while in the length scale of 0.3 μm to 5 μm, the high temperature surface is more uniform than that of the low temperature surface. This conclusion is consistent with the AFM observation. To explain it more clearly, we plot the peak-peak distributions of the two surfaces ($T_s=-50$ °C and 120 °C) in Figs. 7(a) and 7(b), respectively. The images shown in Fig. 7 are obtained from the AFM topographies by the following method: if $h_{ij}>h_{i'+k,j'+k}$, let $h_{ij}=1$ (black spot); otherwise $h_{ij}=0$ (white spot), where h_{ij} is the height of an image pixel and $h_{i'+k,j'+k}(k=0,1)$ are the heights of the four nearest pixels of h_{ij}. From Fig. 7, we can find that the two images are very

FIG. 7. Peak-peak distributions of the surfaces prepared at temperatures of -50 °C (a) and 120 °C (b).

different. For the low temperature surface [Fig. 7(a)], peak-peak distribution shows confusion patterns, but in local regions we can see small white or black areas which indicate the existence of local flat surfaces, while for the high temperature surface [Fig. 7(b)], black spots are randomly distributed and no local flat areas are observed like those in the low temperature surface. The result of Fig. 7 supports the conclusion deduced from the multifractal spectra that spatial distribution of the low temperature surface is relatively flat in small length scale and is rough in large length scale, and the result is reversed for the high temperature surface.

V. CONCLUSION

In summary, we have studied the surface roughness of C_{60}/Ag films grown at different substrate temperatures. The spatial distribution of the surface can be well described by the multifractal spectra. The width and the height of the bell-shaped spectra increase with the increasing of surface roughness. Moreover, the multifractal spectra of low temperature roughening surfaces are different from those of the high temperature surface if the probabilities were calculated in different length scales. Therefore the multifractal spectrum provides an effective way for quantitative analysis of roughness of a nonequilibrium surface.

ACKNOWLEDGMENTS

The program is supported by the National Natural Science Foundation of China (Grant Nos. 59529204 and 19734002), and by the Director Foundation of Chinese Academy of Sciences.

[1] P. R. Nayak, J. Lubr. Technol. **93**, 398 (1971).
[2] F. Family and T. Viscek, J. Phys. A **18**, L75 (1985).
[3] L. Vazques, R. C. Salvarezza, P. Ocon, P. Herrasti, J. M. Vara, and A. J. Arvia, Phys. Rev. E **49**, 1507 (1994).
[4] N. Almquist, Surf. Sci. **355**, 221 (1996).
[5] W. M. Tong, R. Stanley Williams, A. Yanase, Y. Segawa, and M. S. Anderson, Phys. Rev. Lett. **72**, 3374 (1994).
[6] A. Aharony, Physica A **168**, 479 (1990).
[7] Chung-Kung Lee and Shyi-Long Lee, Surf. Sci. **325**, 294 (1995).
[8] T. Vicsek, Physica A **168**, 490 (1990).
[9] H. Li, Z. J. Ding, and Z. Q. Wu, Phys. Rev. B **51**, 13 554 (1995); **53**, 16 631 (1996).
[10] B. Wang, Y. Wang, and Z. Q. Wu, Solid State Commun. **96**, 69 (1995).
[11] Y. Wang, B. Wang, and Z. Q. Wu, Solid State Commun. **103**, 55 (1997).
[12] J. G. Hou, Y. Wang, and W. Xu, Appl. Phys. Lett. **70**, 3110 (1997).
[13] J. G. Hou, Mater. Lett. **34**, 36 (1998).
[14] A. Chhabra and R. V. Jensen, Phys. Rev. Lett. **62**, 1327 (1989).
[15] Hong Yan, David Kessler, and L. M. Sander, Phys. Rev. Lett. **64**, 926 (1990).
[16] Jacques G. Amar and Fereydoon Family, Phys. Rev. Lett. **64**, 543 (1990).
[17] Rong-Fu Xiao and Nai-Ben Ming, Phys. Rev. E **49**, 4720 (1994).